A Closed-Form Likelihood for Particle Filters to Track Extended Objects with Star-Convex RHMs

Jannik Steinbring, Marcus Baum, Antonio Zea, Florian Faion, and Uwe D. Hanebeck

***Abstract*— Modeling 2D extended targets with star-convex Random Hypersurface Models (RHMs) allows for accurate object pose and shape estimation. A star-convex RHM models the shape of an object with the aid of a radial function that describes the distance from the object center to any point on its boundary. However, up to now only linear estimators, i.e., Kalman Filters, are used due to the lack of a explicit likelihood function. In this paper, we propose a closed-form and easy to implement likelihood function for tracking extended targets with star-convex RHMs. This makes it possible to apply nonlinear estimators such as Particle Filters to estimate a detailed shape of a target. We compared the proposed likelihood against the usual Kalman filter approaches with tracking pose and shape of an airplane in 2D. The evaluations showed that the combination of the Progressive Gaussian Filter (PGF) and the new likelihood function delivers the best estimation performance and can outperform the usually employed Kalman Filters.**

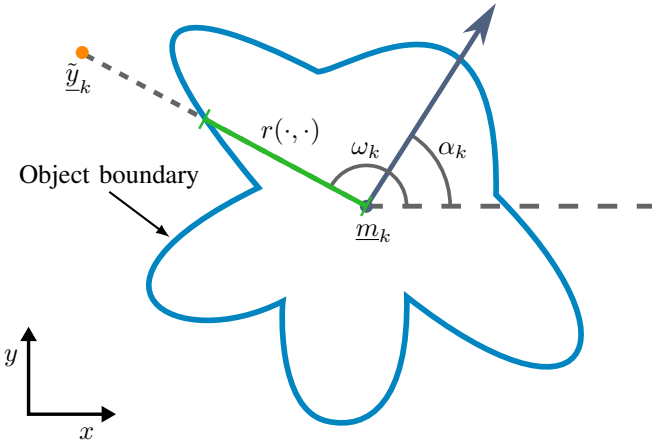

Fig. 1: Star-convex Random Hypersurface Model.

I. Introduction

Object tracking is a fundamental problem in robotics. In this context, the tracking of so-called extended objects gained an increasing interest during the last years [1]. From an extended object, a sensor such as a laser device can receive several noisy measurements in a single scan, where each measurement originates from an unknown source on the object surface. Typically, only very few measurements per scan are available so that it becomes necessary to simultaneously track and estimate the shape of the object. Depending on the specific application, different assumptions on the basic structure of the object shape are a priori suitable. For example, in the presence of high measurement noise it might be suitable to model the object as an ellipse using a random matrix approach [2]. However, in case of rather low noise, a more precise shape description might be feasible. In this context, the so-called Random Hypersurface Model (RHM) was introduced in order to infer star-convex shape approximations using a linear filter [3], [4]. Recently, this approach was further developed in [5] by using Gaussian processes for describing the shape.

For this paper, we will focus on star-convex RHMs, which offer a straightforward mechanism to describe filled shapes, i.e., shapes where measurements also originate from its interior. The idea is to treat the shape interior as a *transformation* of the boundary, or in other words, we describe points in the shape as belonging to an instance of boundary that has been scaled in a certain way. This allows us to reinterpret the problem as a much simpler case of shape fitting for the boundary curve, and we do not need a probabilistic treatment for the whole shape. Furthermore, this also allows the boundary to be arbitrarily detailed without increasing the complexity of the model. Fitting of the boundary can be addressed in three ways. First, a distribution over the measurement sources on the boundary can be assumed [1]. This, however, can be unfavorable if the distribution is incorrect, e.g., due to occlusions. Second, a source can be determined in a greedy way without any distribution in mind [6]. But, for large measurement noise this will cause a bias. Third, a more complex approach based on a so-called partial likelihood can be used which reduces the bias [7]. Here, we make use of the greedy approach as this allows for closed-form solutions. Moreover, estimating a detailed target shape in the presence of large measurement noise is impossible anyway, making the bias problem negligible here.

Usually, extended object tracking is formulated as a nonlinear state estimation problem where the state encompasses the pose and shape parameters of the target. Then, the estimation problem is solved with the aid of a recursive Bayesian estimator. Generally, Bayesian estimators can be divided into two major classes. On the one hand, the class of linear estimators which assume or approximate the nonlinear relationship between state and measurements as a linear function. On the other hand, the class of nonlinear estimators that do not make such linear simplifications.

Up to now, usually linear estimators were used when dealing with star-convex RHMs. In fact, those linear filters have been Kalman Filter derivatives such as the Extended

All authors are with the Intelligent Sensor-Actuator-Systems Laboratory (ISAS), Institute for Anthropomatics and Robotics, Karlsruhe Institute of Technology (KIT), Germany. E-mail: jannik.steinbring@kit.edu, baum@engineer.uconn.edu, antonio.zea@kit.edu, florian.faion@kit.edu, uwe.hanebeck@ieee.org

Kalman Filter (EKF) [8], the Unscented Kalman Filter (UKF) [9], or the Smart Sampling Kalman Filter (S^{2}KF) [10]. They have the advantage that no special treatment for a given measurement model is required in order to use it. However, the explicit or statistical linearization performed by these filters can result in a non-negligible reduction in estimation quality.

On the contrary, nonlinear estimators require an explicit likelihood function. Those must be individually derived for the considered measurement model which can be a demanding task or even impossible. Nevertheless, such a derived likelihood has the advantage that no linearization is required in order to perform the Bayesian measurement update. A popular and well-known class of nonlinear estimators are Particle Filters [11]–[14]. Among these, a promising alternative are filters based on the so-called particle flow approach. Here, the particles are not simply reweighted during a measurement update. Instead, particles are moved through the state space in order to obtain a posterior state estimate. This avoids the inherent sample degeneracy problem of Particle Filters. Such an estimator is for example the Progressive Gaussian Filter (PGF) [15], [16]. Particle Filters for extended object tracking have been developed in [17], [18]. However, the proposed likelihood functions are not available in closed-form for complex shapes.

Therefore, nonlinear estimators have the capabilities to improve the estimation of targets modeled with a star-convex RHM. The missing essential prerequisite, a closed-form and easy to implement likelihood function, will be derived and evaluated against linear filters in this paper. This proposed closed-form solution has the advantages to be more accurate than implementations using numerical integration and is much faster to evaluate. To the best of the authors knowledge, this is the first closed-form likelihood function for target tracking based on star-convex RHMs.

The remainder of this paper is structured as follows. First, we describe the star-convex RHM approach for extended object tracking and formulate the resulting measurement model in Sec. II. Then, in Sec. III, we derive the closed-form likelihood function for the star-convex RHM. In Sec. IV, we evaluate the performance of the proposed closed-form likelihood using two nonlinear filters and compare them with the classical approach based on Kalman Filters by tracking pose and shape of an airplane. Finally, the conclusions are given in Sec. V.

II. Star-Convex Random Hypersurface Models

We consider estimating pose and shape parameters of an extended object in 2D based on noisy point measurements stemming from the object's surface. In this paper, the shape of the object to be tracked is modeled with a star-convex RHM. This model describes the object's shape at a discrete time step k with a radial function $r_k(\phi)$ that specifies the distance from the center of the object

$$\underline{m}_k = [m_k^x, m_k^y]^\top$$

to the boundary point for a given angle $\phi \in [0, 2\pi)$ (see Fig. 1)[1]. The radial function is given as a Fourier series according to

$$r(\underline{c}_k, \phi) = \frac{a_k^{(0)}}{2} + \sum_{j=1}^{F} a_k^{(j)} \cos(j\phi) + b_k^{(j)} \sin(j\phi) \ ,$$

with a fixed number of real coefficients

$$\underline{c}_k = [a_k^{(0)}, a_k^{(1)}, b_k^{(1)}, \ldots, a_k^{(F)}, b_k^{(F)}]^\top \ .$$

Hence, the shape parameters are given by the vector $\underline{c}_k$ of Fourier coefficients [3]. Furthermore, the pose parameters consist of the center $\underline{m}_k$ and orientation α_k. All these parameters of interest are collected in system state vector

$$\underline{x}_k = [\underline{m}_k^\top, \alpha_k, \underline{c}_k^\top]^\top \ . \tag{1}$$

In order to keep track of the system state, we receive measurements over time. A measurement is a noisy point

$$\tilde{\underline{y}}_k = [\tilde{y}_k^x, \tilde{y}_k^y]^\top$$

from the object's surface. It is related to the system state by means of the nonlinear measurement equation

$$\begin{aligned} \underline{y}_k &= \underline{h}(\underline{x}_k, \tilde{\underline{y}}_k, s) + \underline{v}_k \\ &= s \cdot r(\underline{c}_k, \omega_k - \alpha_k) \cdot \begin{bmatrix} \cos(\omega_k) \\ \sin(\omega_k) \end{bmatrix} + \underline{m}_k + \underline{v}_k \ , \end{aligned} \tag{2}$$

with angle

$$\omega_k = \operatorname{atan2}(\tilde{y}_k^y - m_k^y, \tilde{y}_k^x - m_k^x) \ .$$

Here, $\operatorname{atan2}(\cdot)$ denotes the four-quadrant inverse tangent and $\underline{v}_k$ an additive, zero-mean Gaussian white noise term with covariance matrix $\mathbf{R}_k$[2]. It is important to note that the measurement equation explicitly depends upon the received measurement itself. This is due to the greedy approach we chose to determine the unknown source. Moreover, as $r(\cdot, \cdot)$ represents only the object's boundary, the multiplicative noise

$$s = \sqrt{u} \ , \quad u \sim \mathcal{U}(0, 1)$$

scales the radial function to be able to cover all points on the object's surface, not only the points on the boundary [19]. With the fundamental theorem of transforming a random variable [20] and $s = g(u) = \sqrt{u}$ we obtain the probability density density function (PDF) of s according to

$$f^s(s) = \frac{1}{|g'(s^2)|} \mathcal{U}(s^2; 0, 1) = \begin{cases} 2s & , \ s \in [0, 1] \\ 0 & , \text{ elsewhere} \ . \end{cases}$$

Furthermore, it is assumed that s is independent of $\underline{v}_k$. Fig. 1 illustrates the relationship between a received measurement $\tilde{\underline{y}}_k$ and the system state $\underline{x}_k$ defined by the measurement model (2).

Together with a PDF for the initial system state $\underline{x}_0$ and a proper system model describing the temporal evolution of the object's pose and shape, a recursive Bayesian estimator

[1] Vectors are underlined.

[2] Note that $\tilde{\underline{y}}_k$ is a concrete measurement, whereas $\underline{y}_k$ is a random vector.

can be applied to obtain a probability distribution of the system state over time. Linear estimators such the UKF can directly make use the described measurement model. However, nonlinear estimators require an explicit likelihood function instead. Hence, in the following we derive a closed-form likelihood function to be able to track extended objects with a star-convex RHM using nonlinear filters.

III. Closed-Form Likelihood for Star-Convex Random Hypersurface Models

In this section, we consider the measurement update of a recursive nonlinear Bayesian estimator. The update is based on Bayes' rule and is defined as

$$f(\underline{x}_k \,|\, \underline{\tilde{y}}_k) \propto f(\underline{\tilde{y}}_k \,|\, \underline{x}_k) \cdot f(\underline{x}_k) \ ,$$

where the PDF $f(\underline{x}_k)$ denotes the prior state estimate, $f(\underline{\tilde{y}}_k \,|\, \underline{x}_k)$ the likelihood function, and the conditional PDF $f(\underline{x}_k \,|\, \underline{\tilde{y}})$ the posterior state estimate. The likelihood depends upon the measurement model, and hence, has to be individually derived for the concrete estimation problem. For the star-convex RHM (2), the likelihood is given by

$$\begin{aligned} f(\underline{\tilde{y}}_k \,|\, \underline{x}_k) = &\iint \delta(\underline{\tilde{y}}_k - (\underline{h}(\underline{x}_k, \underline{\tilde{y}}_k, s) + \underline{v}_k)) \cdot \\ &\qquad \mathcal{N}(\underline{v}_k; \underline{0}, \mathbf{R}_k) \cdot f^s(s) \,\mathrm{d}\underline{v}_k \,\mathrm{d}s \\ = &\int \mathcal{N}(\underline{\tilde{y}}_k - \underline{h}(\underline{x}_k, \underline{\tilde{y}}_k, s); \underline{0}, \mathbf{R}_k) \cdot f^s(s) \,\mathrm{d}s \end{aligned} \tag{3}$$

The remaining integral *can* be solved in closed-form. Unfortunately, the resulting terms are not very numerically stable making them unsuitable for a robust state estimation. In particular, when dealing this small measurement noise $\mathbf{R}_k$.

Nonetheless, to obtain a numerically stable analytic likelihood function, we approximate the sawtooth-shaped multiplicative noise PDF $f^s(s)$ as a Gaussian using moment matching, that is,

$$f^s(s) \approx \mathcal{N}(s\,; \hat{s}, \sigma_s^2) \ , \tag{4}$$

with mean

$$\hat{s} = \frac{2}{3}$$

and variance

$$\sigma_s^2 = \frac{1}{18} \ .$$

Based on (4), we get an approximation of the likelihood (3) according to

$$\begin{aligned} f_{sc}(\underline{\tilde{y}}_k \,|\, \underline{x}_k) = \int &\mathcal{N}(\underline{\tilde{y}}_k - \underline{h}(\underline{x}_k, \underline{\tilde{y}}_k, s); \underline{0}, \mathbf{R}_k) \cdot \\ &\mathcal{N}(s\,; \hat{s}, \sigma_s^2) \,\mathrm{d}s \ , \end{aligned} \tag{5}$$

which can also be solved analytically.

Theorem 3.1 (Star-Convex RHM Likelihood):
A closed-form solution for the star-convex RHM likelihood function (5) is given by

$$f_{sc}(\underline{\tilde{y}}_k \,|\, \underline{x}_k) = \frac{d_k}{\sqrt{1 + p_k \sigma_s^2}} \cdot \exp\left(-\frac{1}{2} \frac{(\hat{s} - q_k)^2}{(\frac{1}{p_k} + \sigma_s^2)} \right), \tag{6}$$

where

$$\begin{aligned} d_k &= \frac{1}{2\pi\sqrt{|\mathbf{R}_k|}} \exp\left(-\frac{1}{2} \left(z_k - \frac{w_k^2}{p_k} \right) \right) \\ q_k &= \frac{w_k}{p_k} \\ p_k &= \underline{a}_k^\top \mathbf{R}_k^{-1} \underline{a}_k \\ w_k &= \underline{b}_k^\top \mathbf{R}_k^{-1} \underline{a}_k \\ z_k &= \underline{b}_k^\top \mathbf{R}_k^{-1} \underline{b}_k \\ \underline{a}_k &= r(\underline{c}_k, \omega_k - \alpha_k) \cdot \begin{bmatrix} \cos(\omega_k) \\ \sin(\omega_k) \end{bmatrix} \\ \underline{b}_k &= \underline{\tilde{y}}_k - \underline{m}_k \ . \end{aligned}$$

Proof: The proof is given in the Appendix. ∎

Normally, nonlinear filters use or even explicitly require the logarithm of the likelihood function, the so-called log-likelihood, rather than the original likelihood. The logarithm of the star-convex RHM likelihood function (6) is given by

$$\begin{aligned} \log(f_{sc}(\underline{\tilde{y}}_k \,|\, \underline{x}_k)) = &-\log(2\pi) - \frac{1}{2}\log(|\mathbf{R}_k|) \\ &- \frac{1}{2}\left(z_k - \frac{w_k^2}{p_k} \right) \\ &- \frac{1}{2}\log1\mathrm{p}(p_k \sigma_s^2) - \frac{1}{2}\frac{(\hat{s} - q_k)^2}{(\frac{1}{p_k} + \sigma_s^2)} \ , \end{aligned} \tag{7}$$

where $\log1\mathrm{p}(x)$ denotes the more accurate implementation of $\log(1 + x)$ that can be found in the C standard library or Matlab. Note also that the inverse of $\mathbf{R}_k$ and its determinant can be easily computed analytically as $\mathbf{R}_k$ is a 2×2-matrix.

Up to now, we considered only the case when dealing with one measurement per update. However, in many cases a set of L measurements

$$\mathcal{Y}_k = \{\underline{\tilde{y}}_k^{(1)}, \ldots, \underline{\tilde{y}}_k^{(L)}\}$$

is available for processing at a certain time step. Under the assumption that the measurement noises for different measurements $\underline{\tilde{y}}_k^{(i)}$ are mutually independent, the logarithm of the likelihood $f_{sc}(\mathcal{Y}_k \,|\, \underline{x}_k)$ can be efficiently computed according to

$$\log(f_{sc}(\mathcal{Y}_k \,|\, \underline{x}_k)) = \sum_{i=1}^{L} \log(f_{sc}(\underline{\tilde{y}}_k^{(i)} \,|\, \underline{x}_k)) \ . \tag{8}$$

In summary, to track an extended object with a star-convex RHM and multiple measurements per time step the efficient log-likelihood based on (7) and (8) can be used.

IV. Evaluation

We want to assess the performance of the proposed closed-form star-convex RHM log-likelihood function by means of tracking pose, velocities, and shape of an airplane similar to [21] using various linear and nonlinear estimators. The velocities are given by the angular velocity $\dot{\alpha}_k$ and the speed ν_k along the object's heading. Consequently, we extend the system state vector (1) to

$$\underline{x}_k = [\underline{m}_k^\top,\, \alpha_k,\, \nu_k,\, \dot{\alpha}_k,\, \underline{c}_k^\top]^\top \ .$$

For the considered scenario, we use 15 Fourier coefficients, i.e., $F = 14$, to approximate the airplane's shape. Hence, the entire system state is of dimension 20.

The airplane has a wingspread of 100 m and we simulate the airplane's trajectory over 580 time steps as depicted in Fig. 2. The temporal evolution of the airplane is modeled with a nonlinear constant velocity model

$$\begin{aligned}\underline{x}_k &= \underline{a}(\underline{x}_{k-1}, \Delta t) + \underline{w} \\ &= \begin{bmatrix} m^x_{k-1} + \cos(\alpha_{k-1}) \cdot \Delta t \cdot \nu_{k-1} \\ m^y_{k-1} + \sin(\alpha_{k-1}) \cdot \Delta t \cdot \nu_{k-1} \\ \alpha_{k-1} + \Delta t \cdot \dot{\alpha}_{k-1} \\ \nu_{k-1} \\ \dot{\alpha}_{k-1} \\ \underline{c}_{k-1} \end{bmatrix} + \underline{w} \ ,\end{aligned}$$

with $\Delta t = 1$ and additive, zero-mean, and time-invariant Gaussian white noise $\underline{w}$ with covariance matrix

$$\mathbf{Q} = \mathrm{diag}(1, 1, 10^{-7}, 1, 10^{-6}, 10^{-2}, \ldots, 10^{-2}) \ .$$

Moreover, at each time step, we receive a set of 15 noisy measurements

$$\mathcal{Y}_k = \{\tilde{\underline{y}}^{(1)}_k, \ldots, \tilde{\underline{y}}^{(15)}_k\}$$

that are generated uniformly on the airplane's surface. Like the nonlinear filters, the sample-based Kalman filters also process all measurements in a single measurement update by stacking the measurements into a large measurement vector according to

$$\begin{bmatrix} \tilde{\underline{y}}^{(1)}_k \\ \vdots \\ \tilde{\underline{y}}^{(15)}_k \end{bmatrix} = \begin{bmatrix} \underline{h}(\underline{x}_k, \tilde{\underline{y}}^{(1)}_k, s^{(1)}) + \underline{v}^{(1)}_k \\ \vdots \\ \underline{h}(\underline{x}_k, \tilde{\underline{y}}^{(15)}_k, s^{(15)}) + \underline{v}^{(15)}_k \end{bmatrix} \ .$$

Note that the additive noises $\underline{v}^{(i)}_k$ can be handled analytically by the linear filters and do not have to be sampled. Consequently, for the measurement update only a $20 + 15 = 35$ dimensional Gaussian has to be sampled.

Two nonlinear estimators are used to evaluate the proposed log-likelihood function:

1) the Sequential Importance Resampling Particle Filter (SIR-PF) [13] with 50,000 particles, and
2) the Progressive Gaussian Filter (PGF) [15] with 201 samples for the prediction and 401 samples per progression step.

For comparison, we also evaluate two linear estimators that make directly use of the measurement model (2):

1) the Unscented Kalman Filter (UKF) [9] that uses 41 samples for the prediction and 71 samples for the update, and
2) the Smart Sampling Kalman Filter (S^{2}KF) [10] with 201 samples for the prediction and 401 samples for the update.

To investigate the performance of the various estimators for different noise conditions, we consider three different time-invariant isotropic measurement noise levels with covariance

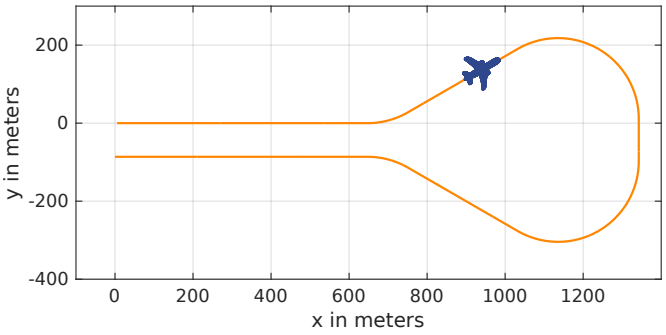

Fig. 2: Trajectory (orange) of the plane to track (blue).

matrices

$$\begin{aligned}\mathbf{R}^l &= 0.1^2\mathbf{I}_2 \\ \mathbf{R}^m &= 1^2\mathbf{I}_2 \\ \mathbf{R}^h &= 10^2\mathbf{I}_2 \ ,\end{aligned}$$

respectively and $\mathbf{I}_2$ is the identity matrix of dimension two.

We perform 50 Monte Carlo runs. In each run, the initial state estimate for all filters is set to a Gaussian distribution with mean

$$\hat{\underline{x}}_0 = [\hat{\underline{y}}^\top, 0, 0, 0, 2d, 0, \ldots, 0]^\top$$

and covariance matrix

$$\mathbf{C}^0 = \mathrm{diag}(\mathbf{C}^y, 10^{-6}, 1, 10^{-6}, 100, 10, \ldots, 10) \ ,$$

where $\hat{\underline{y}}$ denotes the sample mean and $\mathbf{C}^y$ the sample covariance matrix of the first set of available measurements $\mathcal{Y}_0$, and

$$d = \max\left\{\|\hat{\underline{y}} - \tilde{\underline{y}}^{(i)}_0\|_2 : 1 \leq i \leq 15\right\} \ .$$

Hence, the initial airplane shape is initialized as a circle with radius d.

The estimation quality is assessed by computing the average over all Monte Carlo runs of the "Intersection over Union" (IoU) measure [22] between the true airplane shape and the shape estimated by the respective filters[3]. This measure goes from 0 to 1 where a value of 0 means no overlap of the shapes and 1 the shapes are identical and overlap perfectly. Hence, it assesses the quality of both pose and shape parameters.

The results for the three different noise levels are depicted in Figures 3, 4, and 5. For the low noise case, the PGF using the new likelihood attains the best IoU ratio. The SIR-PF is not as good as the PGF, as the small measurement noise results in a narrow likelihood leading to the classical PF problem of sample degeneracy. Both linear filters, and especially the UKF, have more problems estimating pose and shape of the airplane for such small noise. Here, the small noise makes the measurement model more nonlinear, and the performed linearizations only rough approximations. The S^{2}KF with its many samples can mitigate those linearization errors, though. When dealing with the medium noise level, the S^{2}KF and the PGF perform nearly identical whereas the SIR-PF do not reach their accuracy. The UKF has again

[3]For the SIR-PF, we used the particle mean as point estimate.

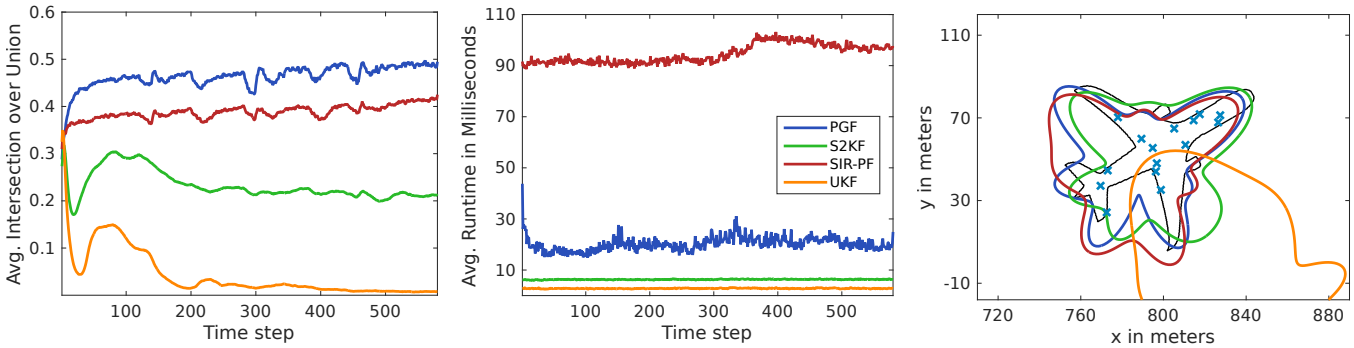

(a) Airplane intersection over union. (b) Measurement update runtimes. (c) Simulation run after 150 time steps.

Fig. 3: Airplane tracking results with low measurement noise ($\mathbf{R}^l$).

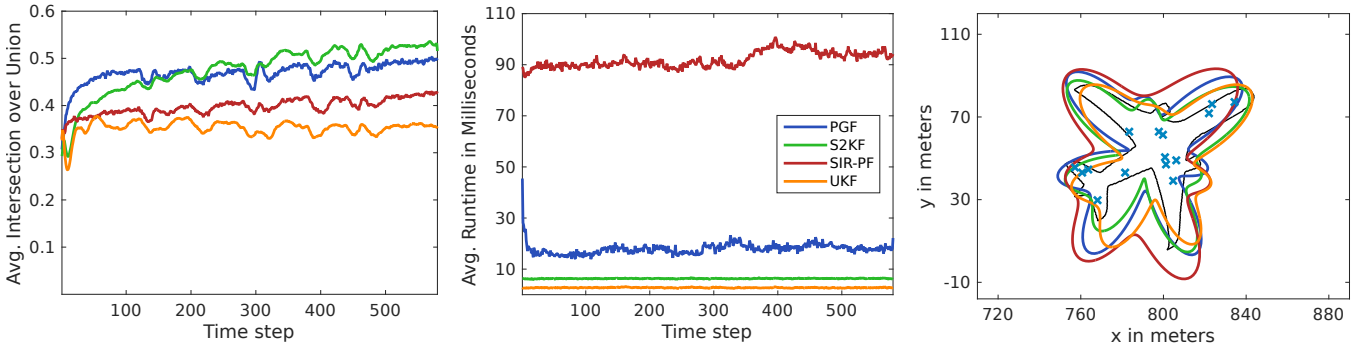

(a) Airplane intersection over union. (b) Measurement update runtimes. (c) Simulation run after 150 time steps.

Fig. 4: Airplane tracking results with medium measurement noise ($\mathbf{R}^m$).

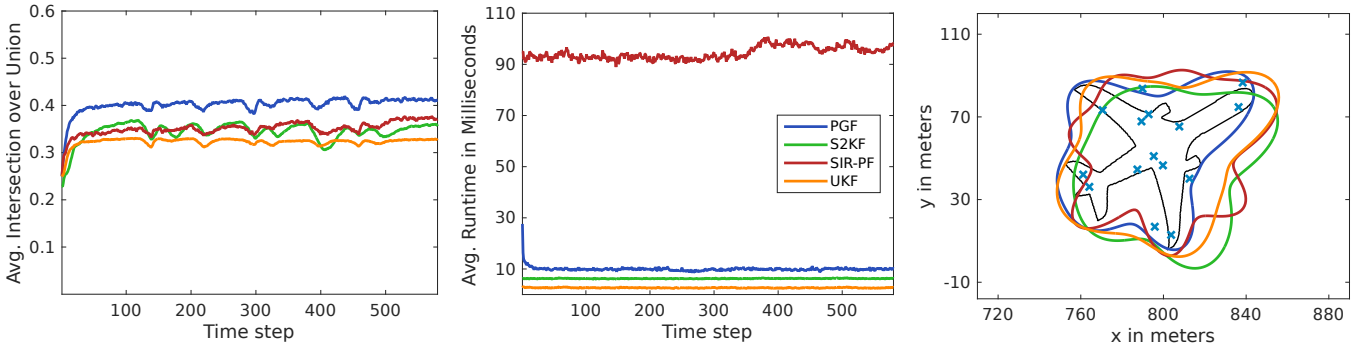

(a) Airplane intersection over union. (b) Measurement update runtimes. (c) Simulation run after 150 time steps.

Fig. 5: Airplane tracking results with high measurement noise ($\mathbf{R}^h$).

the worst estimation results. For the highest measurement noise level, the SIR-PF, the S^2KF, and the UKF perform very similar, whereas the PGF is again the best estimator. Note also that the IoU ratio in general decreases as the large measurement noise prevents a detailed shape estimate.

When looking at the measurement update runtimes of the respective filters, it can be seen that they do not differ much between the various noise levels. As the Kalman Filters always use a constant number of samples, their runtimes are constant over all time steps and different noise levels. Due to the many particles used by the SIR-PF, it needs with approximately 100 ms the longest time for performing an update. In contrast to this, the PGF only initially has some higher runtimes. After a few time steps it converges to a much lower runtime between 30 and 10 ms. It should also be noted that for larger measurement noise the runtimes become much smoother and shorter. All of this can be explained with the adaptive number of progression steps perform by the PGF. For smaller noise, the measurements contain more information about the system state and consequently the likelihood function becomes more spiky. As a result, the filter needs more progression steps to obtain the posterior state estimate.

In summary, the combination of PGF and new closed-form likelihood function offers the best tradeoff between estimation accuracy and runtime across the investigated measurement noise levels.

V. Conclusions

In this paper, we derived a closed-form and easy to implement likelihood function for tracking extended targets with a star-convex Random Hypersurface Model (RHM). First, we described how the extent of an object is modeled by an star-convex RHM and how noisy point measurements from the object's surface are related to it. Then, we derived the closed-form likelihood function and also gave formulas for the $\log$-likelihood required by many nonlinear Bayesian estimators. Finally, we investigated the performance of the proposed closed-form solutions by means of tracking pose, velocities, and shape of an airplane in 2D. Two nonlinear estimators using the new likelihood were compared against two sample-based Kalman filters as those linear filters are currently the means of choice when dealing with star-convex RHMs. The evaluations for different measurement noise levels showed that the combination of Progressive Gaussian Filter (PGF) and new likelihood function delivers the best estimation performance and can outperform the usually employed linear estimators.

Appendix

Our goal is to compute the likelihood function (5) analytically. By defining the vectors

$$\underline{a}_k = r(\underline{c}_k, \omega_k - \alpha_k) \cdot \begin{bmatrix} \cos(\omega_k) \\ \sin(\omega_k) \end{bmatrix}$$

and

$$\underline{b}_k = \underline{\tilde{y}}_k - \underline{m}_k \ ,$$

we get

$$f_{sc}(\underline{\tilde{y}}_k \,|\, \underline{x}_k) = \int \frac{\exp\left(-\frac{1}{2}(\underline{b}_k - s \cdot \underline{a}_k)^\top \mathbf{R}_k^{-1} (\underline{b}_k - s \cdot \underline{a}_k)\right)}{2\pi\sqrt{|\mathbf{R}_k|}} \cdot \mathcal{N}(s\,; \hat{s}, \sigma_s^2)\ \mathrm{d}s \ .$$

With completing the square, we obtain

$$f_{sc}(\underline{\tilde{y}}_k \,|\, \underline{x}_k) = \underbrace{\frac{\exp\left(-\frac{1}{2}\left(\underline{b}_k^\top \mathbf{R}_k^{-1} \underline{b}_k - \frac{(\underline{b}_k^\top \mathbf{R}_k^{-1} \underline{a}_k)^2}{\underline{a}_k^\top \mathbf{R}_k^{-1} \underline{a}_k}\right)\right)}{2\pi\sqrt{|\mathbf{R}_k|}}}_{:= d_k} \cdot \int \exp\Big(-\frac{1}{2} \underbrace{\underline{a}_k^\top \mathbf{R}_k^{-1} \underline{a}_k}_{:= p_k} \Big(s - \underbrace{\frac{\underline{b}_k^\top \mathbf{R}_k^{-1} \underline{a}_k}{\underline{a}_k^\top \mathbf{R}_k^{-1} \underline{a}_k}}_{:= q_k}\Big)^2\Big) \cdot \mathcal{N}(s\,; \hat{s}, \sigma_s^2)\ \mathrm{d}s$$

$$= d_k \sqrt{\frac{2\pi}{p_k}} \cdot \int \mathcal{N}\left(s\,; q_k, p_k^{-1}\right) \cdot \mathcal{N}(s\,; \hat{s}, \sigma_s^2)\ \mathrm{d}s \,.$$

Finally, by exploiting that the product of two Gaussians is also an unnormalized Gaussian and a density function always integrates to one, we yield the final closed-form likelihood

$$f_{sc}(\underline{\tilde{y}}_k \,|\, \underline{x}_k) = \frac{d_k}{\sqrt{1 + p_k \sigma_s^2}} \cdot \exp\left(-\frac{1}{2} \frac{(\hat{s} - q_k)^2}{(\frac{1}{p_k} + \sigma_s^2)}\right) \ .$$

References

[1] K. Gilholm and D. Salmond, "Spatial Distribution Model for Tracking Extended Objects," *IEE Proceedings Radar, Sonar and Navigation*, vol. 152, no. 5, pp. 364–371, Oct. 2005.

[2] Michael Feldmann, Dietrich Fränken, and Wolfgang Koch, "Tracking of Extended Objects and Group Targets Using Random Matrices," *IEEE Transactions on Signal Processing*, vol. 59, no. 4, pp. 1409–1420, Apr. 2011.

[3] Marcus Baum and Uwe D. Hanebeck, "Shape Tracking of Extended Objects and Group Targets with Star-Convex RHMs," in *Proceedings of the 14th International Conference on Information Fusion (Fusion 2011)*, Chicago, USA, Jul. 2011.

[4] ——, "Extended Object Tracking with Random Hypersurface Models," *IEEE Transactions on Aerospace and Electronic Systems*, vol. 50, no. 1, pp. 149–159, Jan. 2014.

[5] Niklas Wahlström and Emre Özkan, "Extended Target Tracking Using Gaussian Processes," *IEEE Transactions on Signal Processing*, Apr. 2015.

[6] Florian Faion, Antonio Zea, and Uwe D. Hanebeck, "Reducing Bias in Bayesian Shape Estimation," in *Proceedings of the 17th International Conference on Information Fusion (Fusion 2014)*, Salamanca, Spain, Jul. 2014.

[7] Florian Faion, Antonio Zea, Marcus Baum, and Uwe D. Hanebeck, "Partial Likelihood for Unbiased Extended Object Tracking," in *Proceedings of the 18th International Conference on Information Fusion (Fusion 2015)*, Washington D. C., USA, Jul. 2015.

[8] Dan Simon, *Optimal State Estimation*, 1st ed. Wiley & Sons, 2006.

[9] Simon J. Julier and Jeffrey K. Uhlmann, "Unscented Filtering and Nonlinear Estimation," in *Proceedings of the IEEE*, vol. 92, Mar. 2004, pp. 401–422.

[10] Jannik Steinbring and Uwe D. Hanebeck, "LRKF Revisited: The Smart Sampling Kalman Filter (S2kf)," *Journal of Advances in Information Fusion*, vol. 9, no. 2, pp. 106–123, Dec. 2014.

[11] Sanjeev Arulampalam, Simon Maskell, Neil Gordon, and Tim Clapp, "A Tutorial on Particle Filters for Online Nonlinear/Non-Gaussian Bayesian Tracking," *IEEE Transactions on Signal Processing*, vol. 50, no. 2, pp. 174–188, Feb. 2002.

[12] Jayesh H. Kotecha and Petar M. Djuric, "Gaussian Particle Filtering," *IEEE Transactions on Signal Processing*, vol. 51, no. 10, pp. 2592–2601, Oct. 2003.

[13] Branko Ristic, Sanjeev Arulampalam, and Neil Gordon, *Beyond the Kalman Filter: Particle Filters for Tracking Applications*. Artech House Publishers, 2004.

[14] Arnaud Doucet and Adam M. Johansen, "A Tutorial on Particle Filtering and Smoothing: Fifteen Years Later," in *Oxford Handbook of Nonlinear Filtering*, 2011, pp. 656–704.

[15] Jannik Steinbring and Uwe D. Hanebeck, "Progressive Gaussian Filtering Using Explicit Likelihoods," in *Proceedings of the 17th International Conference on Information Fusion (Fusion 2014)*, Salamanca, Spain, Jul. 2014.

[16] ——, "GPU-Accelerated Progressive Gaussian Filtering with Applications to Extended Object Tracking," in *Proceedings of the 18th International Conference on Information Fusion (Fusion 2015)*, Washington D. C., USA, Jul. 2015, pp. 1038–1045.

[17] Nikolay Petrov, Lyudmila Mihaylova, Amadou Gning, and Donka Angelova, "A Novel Sequential Monte Carlo Approach for Extended Object Tracking Based on Border Parameterisation," in *Proceedings of the 14th International Conference on Information Fusion (Fusion 2011)*, Chicago, USA, Jul. 2011.

[18] ——, "Group Object Tracking with a Sequential Monte Carlo Method Based on a Parameterised Likelihood Function," 2012.

[19] Marcus Baum, Benjamin Noack, and Uwe D. Hanebeck, "Extended Object and Group Tracking with Elliptic Random Hypersurface Models," in *Proceedings of the 13th International Conference on Information Fusion (Fusion 2010)*, Edinburgh, United Kingdom, Jul. 2010.

[20] Athanasios Papoulis and S. Unnikrishna Pillai, *Probability, Random Variables and Stochastic Processes*, 4th ed. McGraw-Hill, 2002.

[21] Florian Faion, Antonio Zea, Marcus Baum, and Uwe D. Hanebeck, "Symmetries in Bayesian Extended Object Tracking," *Journal of Advances in Information Fusion*, Jun. 2015.

[22] Benjamin Sapp, Chris Jordan, and Ben Taskar, "Adaptive Pose Priors for Pictorial Structures," in *IEEE Conference on Computer Vision and Pattern Recognition (CVPR)*, San Francisco, USA, Jun. 2010, pp. 422–429.